Journal of Earth Science, *Vol. 22*, *No. 2*, *p. 137–142*, *April 2011* *ISSN 1674-487X*
Printed in China
DOI: 10.1007/s12583-011-0165-x

Melt Evolution above a Spontaneously Retreating Subducting Slab in a Three-Dimensional Model

Guizhi Zhu*
Department of Earth Sciences, *Swiss Federal Institute of Technology* (*ETH Zurich*), *CH*-8092 *Zurich*, *Switzerland*
Taras Gerya
Department of Earth Sciences, *Swiss Federal Institute of Technology* (*ETH Zurich*), *CH*-8092 *Zurich*, *Switzerland*; *Adjunct Professor of Geology Department*, *Moscow State University*, 119899 *Moscow*, *Russia*
David A Yuen
Department of Geology and Geophysics and Minnesota Supercomputing Institute, *University of Minnesota*, *Minneapolis*, *MN* 55415, *USA*

ABSTRACT: Dehydration of the subducting slab favors the melting of the surrounding mantle. Water content and melt evolution atop a spontaneously retreating subducting slab are reported in a three-dimensional (3-D) model. We find that fluids, including water and melts in the rocks, vary substantially along the trench, which cannot be found in two-dimensional (2-D) models. Their maxima along the subducting slab are mainly located at about 50 to 70 and 120 to 140 km. Volumetric melt production rate changes spatially and episodically atop the slab, which may reflect the intensity and variations of volcanoes.

KEY WORDS: subduction, water and melt, three-dimensional model.

INTRODUCTION

It is broadly accepted that fluids and melts are two important players that drastically weaken the materials (Karato, 2010, 2008; Karato and Jung, 1998; Blacic, 1972) and dynamics in the subduction zones (Stern, 2004, 2002). As a plate subducts, fluids are released from the subducting slab and hydrate the surrounding asthenosphere, which results in a sharp decrease in density and viscosity of mantle rocks. The overall concept can be widely used to explain the observation of seismic velocity and magmatism (Kimura and Yoshida, 2006; Zhao et al., 2002; Wyss et al., 2001; Zhao, 2001). Furthermore, the fluid and melt processes involving geochemical and geophysical systems and their interactions with mantle wedge flow in subduction zones have been widely investigated in experimental methods (Grove et al., 2006; Hirth and Kohlstedt, 2003; Karato and Jung, 2003; Mysen and Boettcher, 1975) and two-dimensional (2-D) numerical methods (Hebert et al., 2009; Nikolaeva et al., 2008; Conder and Wiens, 2007; Arcay et al., 2005; Gerya and Yuen, 2003a, b; Iwamori, 1998; Peacock, 1990). Zhu et al. (2009) showed three-dimensional (3-D) complex thermochemical plumes and their corresponding integrated melt productivities at the modeled surface. Honda et al. (2010) used 3-D simple models to analyze the influence of water on the mantle flow. However, there is no knowledge about melt distribution inside 3-D natural subduction zone.

This study was supported by the SNF (Nos. 200021-116381/1, 200020-126832/1).

*Corresponding author: guizhi.zhu@erdw.ethz.ch

Manuscript received August 20, 2010.
Manuscript accepted November 18, 2010.

As shown in this conceptual 3-D model (Fig. 1) of melt distribution atop the subducting slab, the fluid released from the subducting slab favors the melting of the surrounding mantle and partially molten rocks with different melt fractions distribute quite inhomogenously. This contributes mostly to the complex structure of thermochemical plumes in the mantle wedge and uneven distribution of volcanic clusters, such as in Northeast Japan (Kimura and Yoshida, 2006) and New Zealand (de Ronde et al., 2007).

In this article, we investigate the spatial and temporal evolution of melt fraction and water content above the subducting slab from a 3-D numerical model for a spontaneously retreating subduction setting. The evolution of melt productivity inside the subduction zone is also investigated.

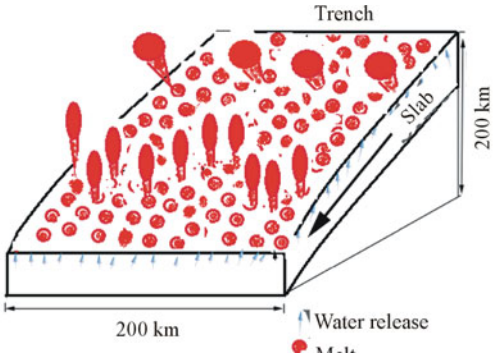

Figure 1. Schematic models for fluids and melts above the subducting slab. Water is released from the subducting slab as shown in blue arrow. Hydrated melts (shown as red filled circles) could form atop the slab and contribute to the volcanic activities.

MODEL DESCRIPTION

The initial setup (808 km long, 200 km wide, and 200 km high, as shown in Fig. 2) of our 3-D numerical petrological-thermomechanical model on intraoceanic spontaneously retreating subduction, where the sinking and retreating of the slab is driven by internal forces only and without any imposed kinematic velocity boundary conditions, is to extend the 2-D model setup (Nikolaeva et al., 2008) along the lateral direction. The oceanic crust consists of a 3-km-thick basaltic overlying 5-km-thick gabbroic rocks. The mantle is composed of anhydrous peridotite. The subduction initiates by a prescribed weak fracture zone (30 km wide and 60 km thick) between two oceanic plates of different ages with 70 and 1 Ma, respectively (Hall et al., 2001). A weak layer (viscosity of 10^{18} Pa·s) at the top of the oceanic crust is used to mimic free surface. Permeable lower boundary, no slip vertical boundary at the sidewall of the old plate side, and free slip boundary for all the rest are used in our model. We use I3ELVIS code, which is based on finite-differences schemes and marker-in-cell techniques combined with multigrid approach (Gerya, 2010), to solve the governing equations of mass, momentum, and temperature. The domain is resolved by 405×101×101 grid points with 30 to 50 million randomly distributed markers. The in-situ rock density is interpolated for every marker at each time step from the look-up density tables (in *P*-*T* space) precomputed with PERPLE_X program for the above rock compositions. Moreover, in order to approximate

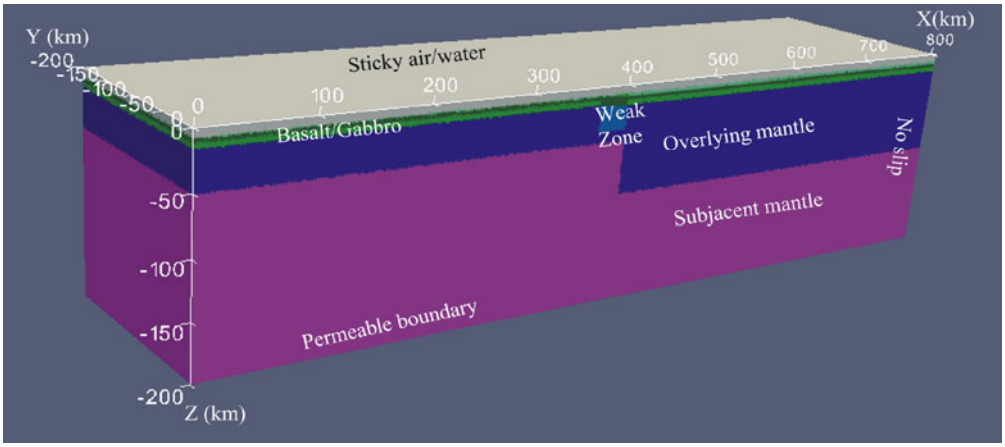

Figure 2. Initial setup of our 3-D numerical petrological-thermomechanical model, which is described in text (see MODEL DESCRIPTION).

the influence of moderate melt extraction, we assume that the maximum of density difference of partially molten rock from solid rock is 300 kg/cm^3.

Dehydration and melting processes are taken into account during the subduction process. According to our model, water released from the slab creates a rheologically weak hydrated zone between the plates that ensures self-sustaining retreating subduction (Gerya et al., 2008). To simulate the migration of water released by dehydration process, we use independently moving rock and fluid markers (Gorczyk et al., 2007). A fluid marker with respective water amount is generated and moves upward until it reaches a lithology that assimilates water, which can account for water transport. An assumed upward speed (10 cm/a) of free water through the mantle is used. The free water is consumed by hydration and melting reactions in the mantle. Consequently, the propagation of the hydration/melting front in the mantle wedge is limited by the availability of water. This propagation is thus related to the rate of subduction, which brings water to depths (Gerya et al., 2006, 2002). The effective viscosity of mantle rocks is calculated as a function of temperature, pressure, and strain rate by using experimentally determined dislocation-creep flow laws (Ranalli, 1995). The viscosity of partially molten rocks was taken to be constant as 10^{19} Pa·s. The volumetric degree of hydrous melting is a linear function of pressure and temperature as shown by Gerya and Yuen (2003a). The detailed description of petrological-thermomechanical model can be obtained in Zhu et al. (2009).

RESULTS

Evolution of Melt Fraction and Water Content above the Subducting Slab

The 3-D thermochemical plume pattern atop the subducting slab varies during the subducting process (Zhu et al., 2009). In Fig. 3, we show the distribution of the melt fraction and water content in the mantle wedge. In reality, variable hydration would permit melting over a range of temperature and water contents (Grove et al., 2006), but we simply assume that the degree of hydrous melting is a linear function of pressure and temperature as in Gerya and Yuen (2003a). At the beginning of subduction (3.31 Ma), the subducting slab plunges with a shallow dip angle (Figs. 3a, 3b). Slab surface is defined by temperature isosurface at 750 ℃ (Plank et al., 2009) shown in white gray in Fig. 3. Isosurface of melt fraction at 0.05 (red) and isosurface of water content at 0.4 wt.% (blue) in Fig. 3 show that melting can occur atop the subducting slab, which is a favorable condition for low viscosity channel atop the slab (Hebert et al., 2009; Nikolaeva et al., 2008). However, we can also notice the fluctuation of melt fraction close to the trench, which indicates the complex small-scale convection and the formation of a cold nose close to the trench. With the deepening of the subducting slab (Figs. 3c, 3d) at a later stage (7.58 Ma) since the calculation of the model, the range of melt and water widens based on the incipient melt; water and melts have more time to propagate away from the subducting slab. Water has two ways to go into the depth and interact with mantle flow, that is, free water is taken into depth with subducting slab and some water is released from the slab. The fluctuation of water and melt even occurs at the deep part of the subducting slab. The pattern of water content is similar to melt fraction pattern, which reflects the role of water to melt occurrence.

It would be quite interesting to obtain an insight into the lateral variation of melt fraction and water content above the slab. In Fig. 4, cross-sections (e.g., shown as the transparent plane) of melt fraction (Figs. 4a, 4c) and water content (Figs. 4b, 4d) above the slab show their lateral variations above the slab. Meanwhile, we can find that the maximum of melt fraction and water content above the slab is located at two depths of 50 to 70 and 120 to 140 km. More water and melts exist at the shallow depth. Water released from the slab hydrates the surrounding mantle rocks and favors the cold plumes atop the cold slab, which is fueled by partial melting of hydrated mantle and subducted oceanic crust (Gerya and Yuen, 2003b). Melting occurs in the conditions of pressure, temperature, and composition, which may be the low-velocity anomalies atop the subducting slab, such as in Northeast Japan (Zhao et al., 2009). The water front is the front of the cold plumes atop the subducting slab, but the maximum of melt fraction is mainly inside the plumes.

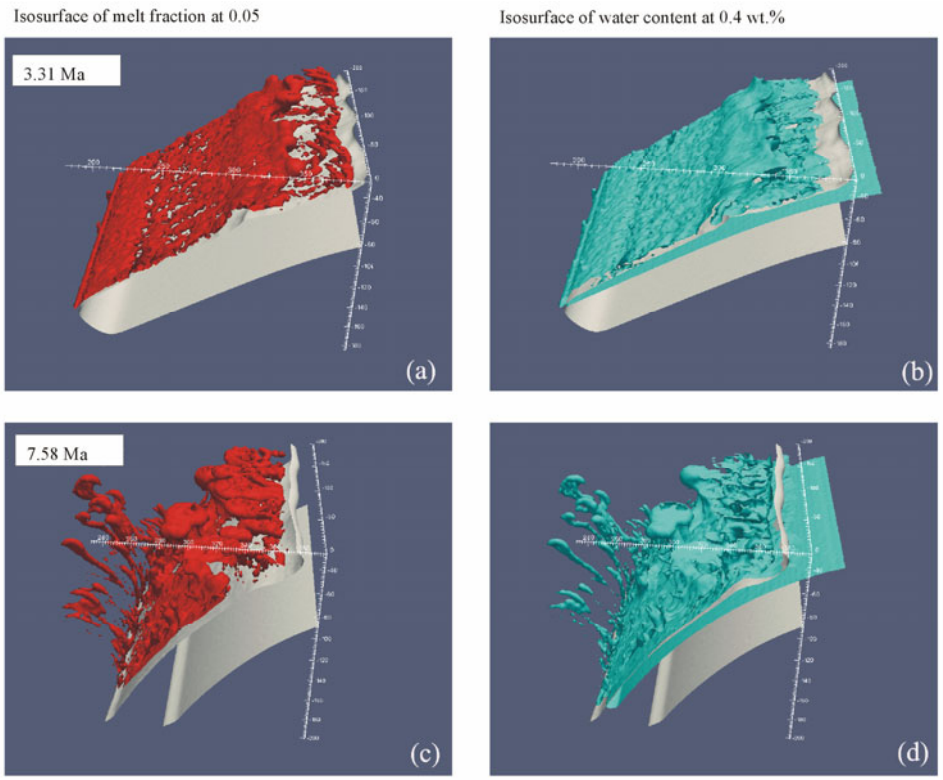

Figure 3. Evolution of melt and water content atop the subducting slab. Isosurface (in red) of melt fraction at 0.05 at 3.31 Ma (a) and 7.58 Ma (c). Isosurface (in blue) of water content at 0.4 wt.% at 3.31 Ma (b) and 7.58 Ma (d). The slab is defined by temperature isosurface at 750 ℃ shown in white gray.

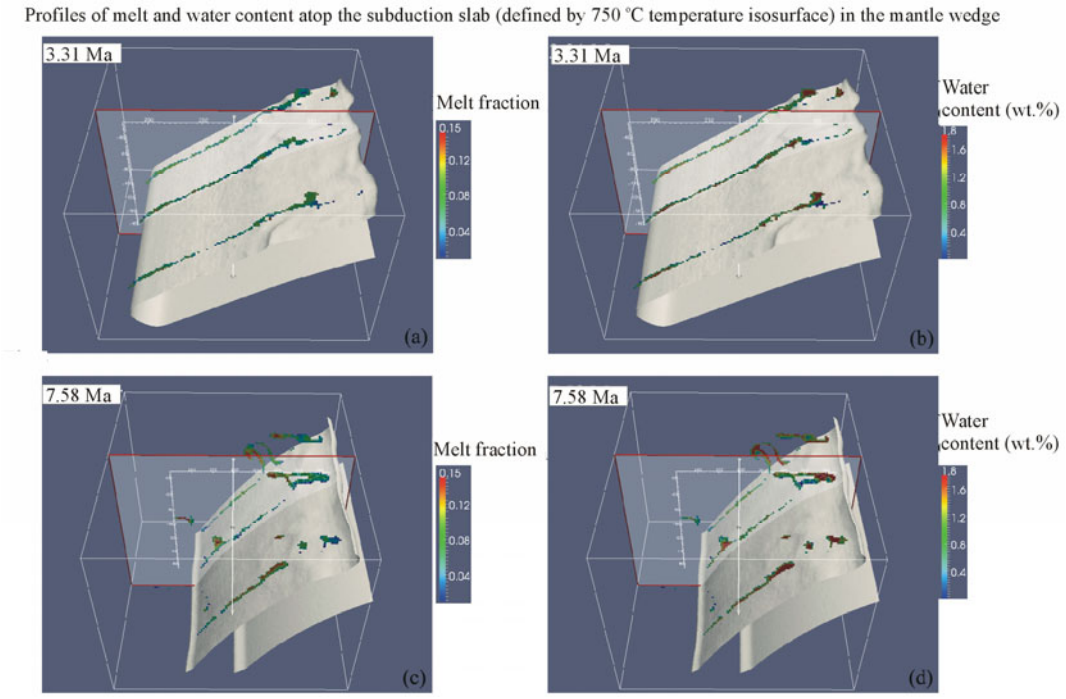

Figure 4. Lateral variation of melts and water content atop the subducting slab. The slab is defined by temperature isosurface at 750 ℃ shown in white gray. Three profiles of melts atop the subducting slab at 3.31 (a) and 7.58 Ma (c) and three profiles of water contents atop the subducting slab at 3.31 (b) and 7.58 Ma (d). Transparent plane shows the location of the middle profile; the scales on the transparent plane show the distance from the surface (vertical scale) and the left end of the model (horizontal scale).

Melt Production Rate atop the Subducting Slab

It is important to analyze the variation of melt production rate in the mantle wedge. In Fig. 5, we show the evolution of volumetric melt production rate (1/Ma) by computing an average Lagrangian time derivative of melt fraction below a given surface area. The 1 250 K temperature isosurface is shown in golden yellow to delineate the top surface of slab (Plank et al., 2009), and volumetric melt production rate above the slab is shown inside the model and two projection planes with color map. These results show that volumetric melt production rate changes spatially and episodically atop the slab. The maximum of volumetric melt production rate appears in the cores of the cold plumes as the result of both decompression and heating of partially molten hydrated rocks composing the plumes. The maximum overall intensity of melt production occurs after the initiation of subduction (Fig. 5a) and then decreases with time (Fig. 5b) because of the cooling of the overlying mantle wedge above the spontaneously retreating slab, but it can increase intermittently with some magnitude (Fig. 5c) later on.

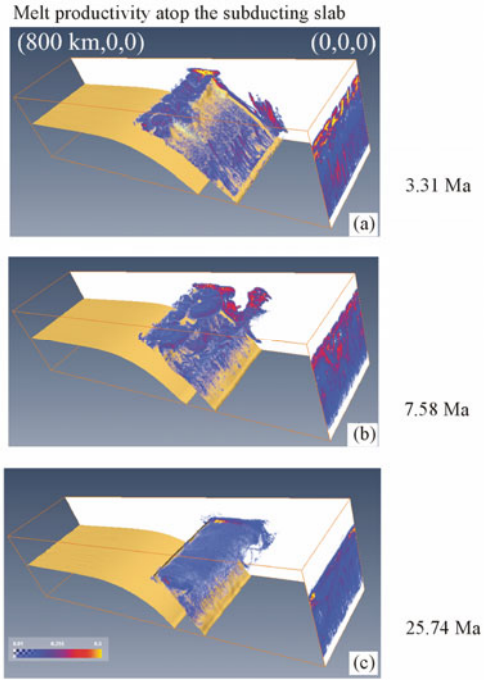

Figure 5. Evolution of melt productivity in the mantle wedge at 3.31 (a), 7.58 (b), and 25.74 Ma (c). Two projection planes are shown in white; the slab surface is defined by temperature isosurface at 1 250 K shown in golden yellow.

DISCUSSION AND CONCLUSIONS

Recently, more and more studies focus on the thermochemical modeling of the mantle wedge because water and melt indeed play important roles in the mantle wedge. However, these models are still in 2-D cases. Our article is the first time to show the evolution of melt/water content above a 3-D spontaneously retreating subducting slab.

There are mainly three messages from our models. (1) Fluids, including water and melts in the rocks, occur above the subducting slab; their maximal is approximately located at two depths: about 50 to 70 and 120 to 140 km. (2) They vary along the trench as well. (3) Volumetric melt production rate changes spatially and episodically atop the slab, which may reflect the intensity and variations of volcanoes as shown by Zhu et al. (2009).

ACKNOWLEDGMENTS

This study was supported by the SNF (Nos. 200021-116381/1, 200020-126832/1). We also thank the “Multiple-Scale Geodynamics of Continental Interiors” workshop.

REFERENCES CITED

Arcay, D., Tric, E., Doin, M. P., 2005. Numerical Simulations of Subduction Zones: Effect of Slab Dehydration on the Mantle Wedge Dynamics. *Phys. Earth Planet. Inter.*, 149(1–2): 133–153

Blacic, J. D., 1972. Effects of Water on the Experimental Deformation of Olivine. In: Heard, H. C., Borg, I. Y., Carter, N. L., et al., eds., Flow and Fracture of Rocks. American Geophysical Union, Washington DC. 109–115

Conder, J. A., Wiens, D. A., 2007. Rapid Mantle Flow beneath the Tonga Volcanic Arc. *Earth Planet. Sci. Lett.*, 264(1–2): 299–307

de Ronde, C. E. J., Baker, E. T., Massoth, G. J., et al., 2007. Submarine Hydrothermal Activity along the Mid-Kermadec Arc, New Zealand: Large-Scale Effects on Venting. *Geochem., Geophys., Geosyst.*, 8: Q07007

Gerya, T. V., 2010. Introduction to Numerical Geodynamic Modelling. Cambridge University Press, Cambridge

Gerya, T. V., Connolly, J. A. D., Yuen, D. A, et al., 2006. Seismic Implications of Mantle Wedge Plumes. *Phys. Earth Planet. Int.*, 156: 59–74

Gerya, T. V., Connolly, J. A. D., Yuen, D. A., 2008. Why is

Terrestrial Subduction One-Sided? *Geology*, 36: 43–46

Gerya, T. V., Stoeckhert, B., Perchuk, A. L., 2002. Exhumation of High-Pressure Metamorphic Rocks in a Subduction Channel: A Numerical Simulation. *Tectonics*, 21(6): 1056. doi: 10.1029/2002TC001406

Gerya, T. V., Yuen, D. A., 2003a. Characteristics-Based Marker-in-Cell Method with Conservative Finite-Differences Schemes for Modeling Geological Flows with Strongly Variable Transport Properties. *Phys. Earth Planet. Inter.*, 140(4): 293–318

Gerya, T. V., Yuen, D. A., 2003b. Rayleigh-Taylor Instabilities from Hydration and Melting Propel 'Cold Plumes' at Subduction Zones. *Earth Planet. Sci. Lett.*, 212(1–2): 47–62

Gorczyk, W., Gerya, T. V., Connolly, J. A. D., et al., 2007. Growth and Mixing Dynamics of Mantle Wedge Plumes. *Geology*, 35: 587–590

Grove, T. L., Chatterjee, N., Parman, S. W., et al., 2006. The Influence of H_2O on Mantle Wedge Melting. *Earth Planet. Sci. Lett.*, 249(1–2): 74–89

Hall, P. S., Kincaid, C., 2001. Diapiric Flow at Subduction Zones: A Recipe for Rapid Transport. *Science*, 292(5526): 2472–2475

Hebert, L. B., Antoshechkina, P., Asimow, P., et al., 2009. Emergence of a Low-Viscosity Channel in Subduction Zones through the Coupling of Mantle Flow and Thermodynamics. *Earth Planet. Sci. Lett.*, 278(3–4): 243–256

Hirth, G., Kohlstedt, D. L., 2003. Rheology of the Upper Mantle and the Mantle Wedge: A View from the Experimentalists. In: Eiler, J. E., ed., Inside the Subduction Factory. American Geophysical Union, Washington DC. 83–105

Honda, S., Gerya, T. V., Zhu, G., 2010. A Simple Three-Dimensional Model of Thermochemical Convection in the Mantle Wedge. *Earth Planet. Sci. Lett.*, 290(3–4): 311–318

Iwamori, H., 1998. Transportation of H_2O and Melting in Subduction Zones. *Earth Planet. Sci. Lett.*, 160(1–2): 65–80

Karato, S. I., 2008. Deformation of Earth Materials: Introduction to the Rheology of the Solid Earth. Cambridge University Press, Cambridge. 463

Karato, S. I., 2010. Rheology of the Earth's Mantle: A Historical Review. *Gondwana Research*, 18(1): 17–45

Karato, S. I., Jung, H. Y., 1998. Water, Partial Melting and the Origin of Seismic Low Velocity and High Attenuation Zone in the Upper Mantle. *Earth Planet. Sci. Lett.*, 157(3–4): 193–207

Karato, S. I., Jung, H. Y., 2003. Effects of Pressure on High-Temperature Dislocation Creep in Olivine. *Poilosophical Magazine A*, 83(3): 401–414

Kimura, J. I., Yoshida, T., 2006. Contributions of Slab Fluid, Mantle Wedge and Crust to the Origin of Quaternary Lavas in the NE Japan Arc. *J. Petrol.*, 47(11): 2185–2232

Mysen, B. O., Boettcher, A. L., 1975. Melting of a Hydrous Mantle: II. Geochemistry of Crystals and Liquids Formed by Anatexis of Mantle Peridotite at High Pressures and High Temperatures as a Function of Controlled Activities of Water, Hydrogen, and Carbon Dioxide. *J. Petrol.*, 16(3): 549–593

Nikolaeva, K., Gerya, T. V., Connolly, J. A. D., 2008. Numerical Modelling of Crustal Growth in Intraoceanic Volcanic Arcs. *Phys. Earth Planet. Inter.*, 171(1–4): 336–356

Peacock, S. M., 1990. Fluid Processes in Subduction Zones. *Science*, 248(4953): 329–337

Plank, T., Cooper, L. B., Manning, C. E., 2009. Emerging Geothermometers for Estimating Slab Surface Temperatures. *Nature Geoscience*, 2(9): 611–615

Ranalli, G., 1995. Rheology of the Earth. 2nd ed.. Chapman and Hall, London. 413

Stern, R. J., 2002. Subduction Zones. *Rev. Geophys.*, 40(4): 1012

Stern, R. J., 2004. Subduction Initiation: Spontaneous and Induced. *Earth Planet. Sci. Lett.*, 226(3–4): 275–292

Wyss, M., Hasegawa, A., Nakajima, J., 2001. Source and Path of Magma for Volcanoes in the Subduction Zone of Northeastern Japan. *Geophys. Res. Lett.*, 28(9): 1819–1822

Zhao, D., 2001. Seismological Structure of Subduction Zones and Its Implications for Arc Magmatism and Dynamics. *Phys. Earth Planet. Inter.*, 127(1–4): 197–214

Zhao, D., Mishra, O. P., Sanda, R., 2002. Influence of Fluids and Magma on Earthquakes: Seismological Evidence. *Phys. Earth Planet. Inter.*, 132(4): 249–267

Zhao, D., Wang, Z., Umino, N., et al., 2009. Mapping the Mantle Wedge and Interpolate Thrust Zone of the Northeast Japan Arc. *Tectonophysics*, 467(1–4): 89–106

Zhu, G., Gerya, T. V., Yuen, D. A., et al., 2009. Three-Dimensional Dynamics of Hydrous Thermal-Chemical Plumes in Oceanic Subduction Zones. *Geochem., Geophys., Geosyst.*, 10: Q11006